

**Supplementary material to:****Seeding, maturation, and propagation of A $\beta$  aggregates in Alzheimer's disease**

*Xiaohang Li*<sup>1,\*</sup> [ORCID 0000-0002-7316-2196](https://orcid.org/0000-0002-7316-2196), *Simona Ospitalieri*<sup>1,\*</sup>, *Tessa Robberechts*<sup>1,\*</sup>, *Linda Hofmann*<sup>2</sup>, *Christina Schmid*<sup>2</sup>, *Ajeet Rijal Upadhaya*<sup>2</sup>, *Marta J. Koper*<sup>1,3,4</sup> [ORCID 0000-0003-2255-6088](https://orcid.org/0000-0003-2255-6088), *Christine A.F. von Arnim*<sup>5,6</sup>, *Sathish Kumar*<sup>7</sup> [ORCID 0000-0002-2792-7047](https://orcid.org/0000-0002-2792-7047), *Michael Willem*<sup>8</sup>, *Kathrin Gnoth*<sup>9</sup>, *Meine Ramakers*<sup>10</sup>, *Joost Schymkowitz*<sup>4,10</sup>, *Frederic Rousseau*<sup>4,10</sup>, *Jochen Walter*<sup>7</sup> [ORCID 0000-0002-4678-2912](https://orcid.org/0000-0002-4678-2912), *Alicja Ronisz*<sup>1</sup> [ORCID 0000-0002-4310-0445](https://orcid.org/0000-0002-4310-0445), *Karthikeyan Balakrishnan*<sup>2,11</sup>, *Dietmar Rudolf Thal*<sup>1,2,12</sup> [ORCID 0000-0002-1036-1075](https://orcid.org/0000-0002-1036-1075)

\*These authors contributed equally to this work, the names are listed in alphabetical order

**Author affiliations:**

<sup>1</sup>Department of Imaging and Pathology – Laboratory of Neuropathology, and Leuven Brain Institute KU-Leuven, Leuven, Belgium

<sup>2</sup>Institute of Pathology – Laboratory of Neuropathology, Ulm University, Ulm, Germany

<sup>3</sup>Laboratory for the Research of Neurodegenerative Diseases, Department of Neurosciences, KU Leuven (University of Leuven), Leuven Brain Institute (LBI), Leuven, Belgium

<sup>4</sup>Center for Brain & Disease Research, VIB, Leuven, Belgium

<sup>5</sup>Department of Neurology, Ulm University, Ulm, Germany

<sup>6</sup>Division of Geriatrics, University Medical Center Göttingen, Göttingen, Germany

<sup>7</sup>Department of Neurology, University of Bonn, Bonn, Germany

<sup>8</sup>Chair of Metabolic Biochemistry, Biomedical Center (BMC), Faculty of Medicine, Ludwig-Maximilians-University Munich, 81377 Munich, Germany

<sup>9</sup>Department of Drug Design and Target Validation, Fraunhofer Institute for Cell Therapy and Immunology, Halle, Germany

<sup>10</sup>Switch Laboratory, Department of Cellular and Molecular Medicine, KU Leuven, 3000 Leuven, Belgium

<sup>11</sup>Department of Gene Therapy, Ulm University, Ulm, Germany

<sup>12</sup>Department of Pathology, UZ-Leuven, Leuven, Belgium

**Supplementary methods:***Neuropathology*

The phase of A $\beta$  plaque pathology (A $\beta$  phase) was assessed after screening the A $\beta$ -stained sections for plaque distribution according to previously published protocols<sup>1</sup>: Phase 0 = no amyloid plaques are detected in the brain; phase 1: single amyloid plaques occur exclusively in neocortical brain regions; phase 2: amyloid plaques occur in neocortical and allocortical brain regions, including hippocampus and amygdala; phase 3: in addition to neo- and allocortical regions amyloid plaques occur in the basal ganglia, the thalamus and the hypothalamus; phase 4: additional amyloid plaques can be stained in the midbrain and the inferior olivary nucleus; and phase 5: amyloid plaques can be found in all brain regions including pons and cerebellum which are spared in the lower phases. In this context, staining of one single amyloid plaque with a highly sensitive A $\beta$  antibody (e.g., anti-A $\beta$ <sub>17-24</sub>; Suppl. Tab. 5) indicated that a given anatomical brain region was considered as amyloid positive<sup>1,2</sup>. Braak NFT staging was performed based on sections stained with an antibody against abnormal  $\tau$ -protein according to a widely accepted protocol<sup>3</sup>: Braak NFT stage 0: no abnormal  $\tau$ -protein containing neurons in the entorhinal/transentorhinal cortex; stage I: single neurons in the transentorhinal region exhibit abnormal  $\tau$ -containing neurons; stage II: neurons of the entorhinal region and/or the CA1 and CA2 sectors of the hippocampus develop neuronal  $\tau$  pathology; stage III: neurons of the fusiform and lingual gyrus become abnormally  $\tau$ -positive as well as neurites terminating in the outer molecular layer of the fascia dentata; stage IV:  $\tau$  pathology extends to neurons of the entire temporal neocortex including the superior temporal gyrus; stage V: abnormal  $\tau$ -protein pathology is widespread throughout the entire cortex, only primary cortical areas such as the primary visual cortex remain free of these lesions; stage VI: in the endstage  $\tau$  pathology is also neuropathologically observed in the primary cortical brain regions. The consortium to establish a registry for AD (CERAD) scores for neuritic plaque density were assessed

neuropathologically based on neocortex sections stained with an antibody against abnormal  $\tau$ -protein<sup>4</sup>: CERAD score 0: no neuritic plaques; score 1: single/few neuritic plaques; score 2: moderate number of neuritic plaques; score 3: high number of neuritic plaques. The stage of the topographical expansion of cerebral amyloid angiopathy (CAA) had been assessed as previously described<sup>5</sup>. In short: CAA stage 0 = no CAA; CAA stage 1 = CAA restricted to leptomeningeal and cortical blood vessels of neocortical regions; CAA stage 2 = CAA in leptomeningeal and cortical blood vessels of neocortical, allocortical and cerebellar regions; CAA stage 3 = CAA extends into subcortical nuclei, white matter and/or the brain stem.

To assess the quantitative aspect of A $\beta$  plaque pathology, neocortical A $\beta$ -loads were determined in all cases as the percentage of the area in the temporal neocortex (Brodmann area 36) covered by A $\beta$  plaques detected with anti-A $\beta$ <sub>17-24</sub> (Suppl. Tab. 5). Morphometry for neocortical A $\beta$  load determination was performed using ImageJ image processing and analysis software (National Institutes of Health, Bethesda, USA). For plaque measurements, the area of the morphologically identified plaques was interactively delineated with a cursor and then measured. Neuronal staining by the anti-A $\beta$ <sub>17-24</sub> antibody was considered as cross-reactivity with amyloid precursor protein (APP) and not included for the assessment of the A $\beta$  load. The areas of all plaques in a given cortical region were summed up. The area of the respective cortex areas was likewise measured by interactive delineation with a cursor. The A $\beta$  load was calculated as the percentage of the area of interest covered by A $\beta$  plaques<sup>6</sup>. Accordingly, we determined the allocortical A $\beta$  load in the cingulate gyrus (Brodmann area 24), the striatal A $\beta$  load in the putamen, and the cerebellar A $\beta$  loads in the cerebellar cortex. Likewise, A $\beta$ <sub>N3pE</sub> and A $\beta$ <sub>pSer8</sub> loads were assessed. To document qualitative changes in the aggregate composition, the neuropathological stage of maturation of A $\beta$  plaques (B-A $\beta$  plaque stage) was determined separately for all four investigated brain regions. To do so, sections were immunostained with antibodies raised against A $\beta$ <sub>17-24</sub>, A $\beta$ <sub>N3pE</sub>, and A $\beta$ <sub>pSer8</sub> (Suppl. Tab. 5). Four B-A $\beta$  plaques stages were

distinguished: B-A $\beta$  plaque stage 0 = no A $\beta$  plaques; B-A $\beta$  plaque stage 1 = detection of A $\beta$  plaques that lack immunoreactivity with anti-A $\beta_{N3pE}$ , and anti-A $\beta_{pSer8}$ ; B-A $\beta$  plaque stage 2 = detection of A $\beta$  plaques with antibodies against non-modified epitopes and anti-A $\beta_{N3pE}$  but not anti-A $\beta_{pSer8}$ ; B-A $\beta$  plaque stage 3 = A $\beta$  plaques are detected with all antibodies directed against A $\beta$  and its modified forms, including A $\beta_{pSer8}$ <sup>7</sup>.

### *Biochemistry*

Protein extraction and sample pretreatment for the quantitative and semi-quantitative analysis of A $\beta$ , A $\beta_{N3pE}$ , and A $\beta_{pSer8}$ : Protein extraction was carried out from 38 cases that were already included in previous studies<sup>7,8</sup>. In short, protein extraction for biochemical analysis of A $\beta$  maturation was carried out by using fresh frozen frontal neocortex (Brodmann area 6), cingulate gyrus (Brodmann area 24), putamen, and the cerebellum from cases listed in Suppl. Tab. 1a (Suppl. Fig. 1a, d).

For *quantitative biochemical analysis* (sandwich enzyme-linked immunoassay, sandwich ELISA), 20 mg of brain tissue was homogenized in cold Tris-buffer with protease and phosphatase inhibitors (Halt™ Protease and Phosphatase Inhibitor Cocktail, ThermoFisher Scientific). We sonicated the samples in bioruptor™ Next Gen (Diagenode) at high power and 4 °C. Formic acid was added to the homogenized brain tissue to a final concentration of 70%. After 15 min of incubation on ice and mixing every 5 min, the samples were neutralized by addition of 1 M Tris base supplemented with protease inhibitor cocktail. The extracts were cleared by centrifugation (16100 × g for 15 min at 4 °C) and the supernatants were analyzed by sandwich ELISAs (Suppl. Fig. 1d).

To measure the A $\beta$  concentration of the brain lysates used to induce seeding in the mouse brains, we proceeded accordingly after adding formic acid.

For the *semi-quantitative biochemical analysis* (western blot), 0.4 g of tissue sample was homogenized in 2 ml of 0.32 M sucrose dissolved in Tris-buffered saline (TBS) containing a protease and phosphatase inhibitor-cocktail (Complete and PhosSTOP, Roche, Mannheim, Germany) (Suppl. Fig. 1d). The tissue was first homogenized with Micropestle (Eppendorf, Hamburg, Germany) followed by sonication (Sonoplus HD 2070, Heidolph instruments, Germany). The homogenate was centrifuged for 30 minutes at 14000 x g at 4 °C. The supernatant (s1) was ultracentrifuged at 175000 x g to separate the soluble fraction (supernatant s2) and the dispersible fraction (pellet p2). The pellet (p2) resuspended in TBS and the supernatant as the soluble fraction (s2) were stored at -80 °C until further use, respectively. The pellet (p1) containing the membrane-associated and the solid plaque-associated fraction was resuspended in TBS containing 2% sodium dodecyl sulfate (SDS) was centrifuged at 14000 x g. The supernatant (s3) was kept as membrane-associated SDS soluble fraction. The pellet (p3) was further dissolved in 70% formic acid and the homogenate was lyophilized by centrifuging in the vacuum centrifuge (Vacufuge; Eppendorf, Germany) and reconstituted in 100 µl of 2X lithium dodecyl sulfate (LDS) sample buffer (Invitrogen, Carlsbad, CA, USA) followed by heating at 70°C for 5 minutes. The resultant sample was considered as plaque-associated, formic acid-soluble fraction (Suppl. Fig. 1d)<sup>9</sup>. The total protein contents of soluble, dispersible, and membrane-associated fractions were determined using BCA Protein Assay (Bio-Rad, Hercules, CA, USA).

The assessment of the biochemical stages of A $\beta$  aggregation (B-A $\beta$  stages) was performed as previously published.<sup>7</sup> In short, we detected the presence/absence of A $\beta$ , A $\beta$ <sub>N3pE</sub>, and A $\beta$ <sub>pSer8</sub> in at least one of the four temporal neocortex fractions according to a previously published protocol: B-A $\beta$  stage 0 = no A $\beta$  detectable; B-A $\beta$  stage 1 = detection of A $\beta$  that lacks immunoreactivity with anti-A $\beta$ <sub>N3pE</sub>, and anti-A $\beta$ <sub>pSer8</sub>; B-A $\beta$  stage 2 = detection of A $\beta$  with antibodies against non-modified epitopes and anti-A $\beta$ <sub>N3pE</sub> but not with anti-A $\beta$ <sub>pSer8</sub>; B-A $\beta$  stage

3 = A $\beta$  is detected with all antibodies directed against A $\beta$  and its modified forms, including A $\beta$ <sub>pSer8</sub><sup>7</sup>.

Sandwich enzyme-linked immunoassay (ELISA): Supernatants were diluted as necessary in dilution buffers supplied with the ELISAs (human A $\beta$ <sub>1-40</sub> and A $\beta$ <sub>1-42</sub>: ELISA kits from ThermoFisher Scientific). The assays were carried out according to the manufacturer's instructions. The absorbance was measured at 450 nm by SpectraMax iD3 (Molecular Devices). Standard curves were obtained to document the sensitivity of the ELISAs (Suppl. Fig. 1c).

The supernatants were also analyzed in an in-house sandwich ELISA specific for the A $\beta$ <sub>N3pE</sub>. Thermo Scientific™ clear flat-bottom immuno nonsterile 96-well plates (ThermoFisher Scientific) were coated with capture anti-human A $\beta$ <sub>N3pE</sub> antibody clone J8<sup>10</sup> (gift from Fraunhofer Institute Halle, Germany, 1mg/ml) diluted 1:500 in PBS for 2 h at 37 °C. Wells were drained, washed twice in wash buffer (PBS/0.05%Tween-20) and blocked for 2 h at 37 °C with 300  $\mu$ l of Pierce protein-free PBS blocking buffer (Thermo Scientific). During this incubation, the standards and samples were prepared. A seven-point standard curve was prepared using two-fold serial dilutions of synthetic A $\beta$ <sub>N3pE-40</sub> (Anaspec) in the dilution buffer (Pierce™ protein-free T20 (TBS) blocking buffer (ThermoFisher Scientific)) containing protease and phosphatase inhibitor cocktail to prevent degradation of A $\beta$ <sub>N3pE</sub> (Suppl. Fig. 1c). After two washes, diluted standards and samples were loaded in duplicate along with blanks of dilution buffer and incubated overnight at 4 °C. The following day, after a further three-time wash step, wells were incubated for 2 h at 37 °C with biotinylated anti-A $\beta$  antibody (clone 4G8, biolegend) diluted 1:4000 in the dilution buffer. After three washes, HRP-conjugated streptavidin (ThermoFisher Scientific) was diluted 1:4000 in the dilution buffer and loaded to each well. Finally, four washes were applied before 1-Step™ ultra TMB-ELISA substrate solution (ThermoFisher Scientific) was used as the chromogenic solution, and 2N sulfuric acid (Sigma) was used to stop the reaction after 30 incubation in the dark at room temperature. The

absorbance was measured at 450 nm by SpectraMax iD3 (Molecular Devices). Linearity of dilution was tested and  $A\beta_{1-40}$  and  $A\beta_{pSer8\ 1-40}$  were used to test specificity of this assay.

For the quantification of  $A\beta_{pSer8}$ , the supernatants were analyzed in an in-house sandwich ELISA specific for the  $A\beta_{pSer8}$ . Thermo Scientific™ clear flat-bottom immuno nonsterile 96-well plates (ThermoFisher Scientific) were coated with capture anti-human  $A\beta_{pSer8}$  antibody clone 1E4E11<sup>11</sup> (1mg/ml) diluted 1:500 in PBS and left for 2 h at 37 °C. Wells were drained, washed twice in wash buffer (PBS/0.05%Tween-20) and blocked for 2 h at 37 °C with 300  $\mu$ l of Pierce protein-free PBS blocking buffer (Thermo Scientific). During this incubation, the standards and samples were prepared. A seven-point standard curve was prepared using two-fold serial dilutions of synthetic  $A\beta_{pSer8\ 1-40}$  (PSL GmbH, Heidelberg, Germany) in the dilution buffer (Pierce™ protein-free T20 (TBS) blocking buffer (ThermoFisher Scientific)) containing protease and phosphatase inhibitor cocktail to prevent degradation of  $A\beta_{pSer8}$  (Suppl. Fig. 1c). After two washes, diluted standards and samples were loaded in duplicate along with blanks of dilution buffer and incubated overnight at 4 °C. The following day, after a further three-time wash step, wells were incubated on a horizontal shaker set at 50 rpm for 2 h at 37 °C with HRP-conjugated anti- $A\beta$  antibody (clone 4G8, biolegend) diluted 1:6000 in the dilution buffer. After four washes, the plates were washed and 100  $\mu$ l of biotinylated Tyramide (10  $\mu$ l/ml in amplification diluent concentrate diluted 1:1 with ddH<sub>2</sub>O, ELAST ELISA amplification system, PerkinElmer) was added to each well for 15 minutes at room temperature. After washing, wells were incubated with streptavidin–HRP (100  $\mu$ l/well, concentration of 2  $\mu$ l/mL, ELAST ELISA amplification system, PerkinElmer) in the dilution buffer (Pierce™ protein-free T20 (TBS) blocking buffer (ThermoFisher Scientific)) for 30 minutes at room temperature. Finally, four washes were applied before 1-Step™ ultra TMB-ELISA substrate solution (ThermoFisher Scientific) was used as the chromogenic solution, and 2N sulfuric acid (Sigma) was used to stop the reaction after 30 min incubation in the dark at room temperature. The

absorbance was measured at 450 nm by SpectraMax iD3 (Molecular Devices). A $\beta_{1-40}$  and A $\beta_{N3pE-40}$  were used to test specificity of this assay. Each sample was analyzed in duplicate.

Semi-quantitative biochemical analysis (western blot): Fractions were subjected to SDS-polyacrylamide gel electrophoresis (SDS-PAGE) and subsequent western blot analysis with anti-A $\beta_{1-16}$ , anti-A $\beta_{N3pE}$  and anti-A $\beta_{pSer8}$  antibodies (Suppl. Tab. 5). Blots were developed with an ECL detection system (SuperSignal™ West Dura Extended Duration Substrate and SuperSignal™ West Pico PLUS Chemiluminescent Substrate, ThermoScientific-Pierce, Waltham, MA, USA) and illuminated in ECL Hyperfilm (GE Healthcare, Buckinghamshire, UK, for non-injecting samples) or Amersham Imager 600 (GE Healthcare, Buckinghamshire, UK, for injecting samples). For quantitative comparison of optical densities of the 4 kDa A $\beta$  bands were measured using ImageJ software (NIH, Bethesda, USA) as previously described<sup>6</sup>.

#### *In vitro seeding assay*

Sarkosyl extraction on brain tissue: 50 mg tissue was homogenized in 800  $\mu$ l cold homogenization buffer (10 mM Tris-HCl pH 7.4, 0.8 M NaCl, 1 mM EGTA and 10% sucrose) with a FastPrep (MP Biomedicals) in Lysing Matrix D vials (MP Biomedicals). The homogenate was centrifuged for 20 min at 20,000 x g at 4°C and the pellet was re-dissolved in 500  $\mu$ l homogenization buffer. Universal Nuclease (Pierce) was added, followed by a 30 min incubation at room temperature. The sample was brought to 1% Sarkosyl (Sigma) and incubated for 1h at room temperature while shaking at 400 rpm, followed by centrifugation at 350,000 x g for 1h at 4°C. The pellet was washed once with PBS, then resuspended in 50  $\mu$ l PBS (thus, 1  $\mu$ l PBS per 1 mg starting tissue).

Total A $\beta_{42}$  ELISA on brain sarkosyl-insoluble fractions: The total A $\beta_{42}$  concentration in the sarkosyl-insoluble fractions was determined using human A $\beta_{1-42}$  ELISA kit (Invitrogen). For this, the fractions were brought to 5M Guanidine-HCl. Fractions were then sonicated for 15



min (30 sec on, 30 sec off at 10°C) with a Bioruptor Pico (Diagenode) and incubated for 3h at room temperature. Fractions were diluted 1:10 with PBS, then 1:20 with the diluent of the kit. The ELISA was then performed according to the manufacturer's protocol.

A $\beta$  seeding assay: For this assay, the biosensor mCherry-A $\beta$ <sub>1-42</sub> HEK293T cell line described in Konstantoulea et al., was used.<sup>12</sup> Cells were maintained in DMEM medium, supplemented with 10% FBS, 1 mM sodium pyruvate and non-essential amino acids (all from Gibco), under an atmosphere of 5% CO<sub>2</sub> at 37°C. Cells were plated at a density of 5000 cells per well in 96-well PhenoPlates (PerkinElmer) coated with poly-L-lysine (Sigma). Cells were allowed to attach for 4h, followed by transfection using Lipofectamine 3000 (Invitrogen). For this, the brain sarkosyl-insoluble fractions were first sonicated for 15 min (30 sec on, 30 sec off at 10°C) with a Bioruptor Pico (Diagenode). Then, a volume of 5  $\mu$ l of brain sarkosyl-insoluble fraction was added to a mixture of 0.3  $\mu$ l of Lipofectamine 3000 with 4.7  $\mu$ l of Opti-MEM medium (Gibco). After a 15 min incubation at room temperature, 10  $\mu$ l of mixture was added per well. 72h after transfection, the cells were fixed with methanol. For this, the cell medium was replaced with 100% ice-cold methanol. The plates were incubated for 15 min on ice, then washed three times with PBS. The nuclei of the cells were stained with DAPI (ThermoFisher) following the manufacturer's protocol. Imaging was done at the VIB Screening Core/C-BIOS, using an Opera Phenix HCS high-content screening microscope (PerkinElmer) equipped with filters to detect DAPI (Ex:405 Em:430) and mCherry (Ex:530, Em:560). For each well, 16 fields were imaged at 40X magnification. Image storage and cell segmentation analysis was performed using the Columbus Plus digital platform (PerkinElmer). Nuclei were detected with DAPI. Cytoplasm was detected using background mCherry signal. mCherry-intensive spots were measured, then A $\beta$  seeding was quantified by counting the percentage of spot-containing cells. For the nonAD 10 case, the wells incubated with the highest concentration of brain sarkosyl-insoluble fraction were excluded from analysis due to cell toxicity. Data were analyzed

using Prism 9 (GraphPad Software, US), and non-linear fit [Agonist vs. response (three parameters)] was used to estimate the EC50 of the seeding potency.

### *Animal housing*

Mice were bred by continuous backcrossing of heterozygous males with wild-type females on a C57BL/6 background and housed in Specific Pathogen Free (SPF) facility. The facility provided 12-hour light/dark cycles and a room temperature of 18 to 21°C. The bedding was changed on the same day of every week. Cage enrichment, including cotton balls that mice could use for making a nest, was provided to all cages. All mice were kept in groups of maximum five animals during the experiment. No pretreatments were applied. The animals' health was regularly monitored. The sample size was estimated prior and confirmed post-hoc by an online sample size calculator (<https://www.bu.edu/researchsupport/compliance/animal-care/working-with-animals/research/sample-size-calculations-iacuc/>) with an alpha level at 0.05 and a power of 80 - 90%. The experimental procedures were approved by the ethical committee for animal experimentation (ECD) with project number P125/2016 and carried out according to the Belgian law. We collected and registered residual tissue and unstained slides of the mice from this experiment and created a mouse biobank to allow further analyses of the seeded plaques. We communicated this strategy as a 3Rs method for reducing the number of animals experiments at <https://www.re-place.be/method/biobanking-processed-mice-brains>.

### *Stereotactic injection*

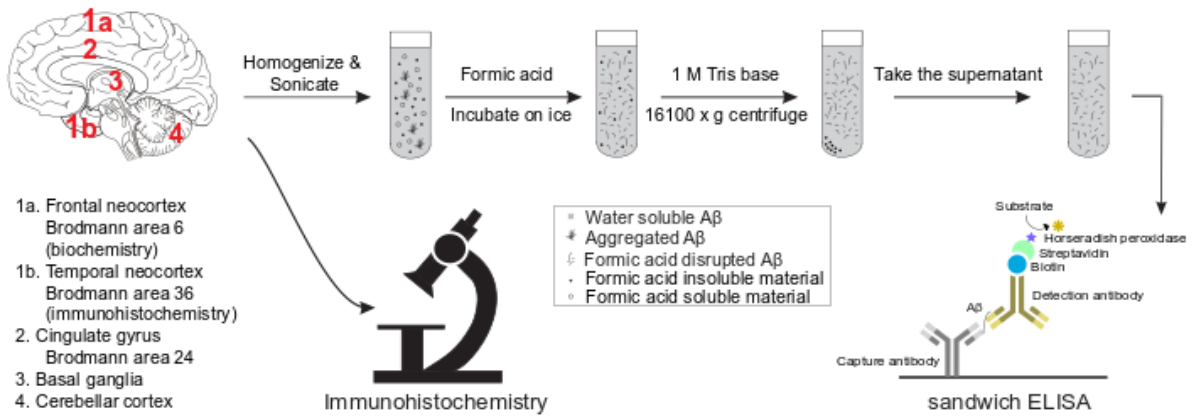
Sixty-nine female APP23 transgenic mice were used and randomly distributed over 11 groups (n= 6-7 for each group) receiving brain extracts from different cases or PBS as indicated in Fig 2c, d. Littermates were randomly assigned to different groups. The body weight of mice assigned to each group was summarized in Suppl. Tab. 6. Overall, body weights ranged between

15.9 – 22.5 g (mean: 19.25 g) before the surgery (at 2 months of age) and 20 – 29.8 g (mean: 23.4 g) at the endpoint of the experiment (at 6 months). Stereotactic injection was carried out every Monday between 8 am and 10 am in an operation room of the animal facility. Before the surgery, two-month-old mice were anaesthetized by intraperitoneal (i.p.) injection of Ketamine (75 mg/kg body weight) and Medetomidine (1 mg/kg body weight). After placing the mice in a stereotactic frame (72-6049, Harvard Apparatus, Massachusetts, USA), one microliter of brain extract was injected in the left hippocampal formation (Bregma: -2.5 mm AP, +2 mm LR, -1.8 mm DV) using a 10  $\mu$ l syringe with a Hamilton needle. One mouse got injected into the right hippocampal formation (Bregma: -2.5 mm AP, -2 mm LR, -1.8 mm DV). The injection was performed at a speed of 1  $\mu$ l/min. We used a separate needle and syringe for each treatment group. Gloves and lab clothing were always worn throughout the procedure. No severe adverse events were observed from any mice of any groups in our experiments.

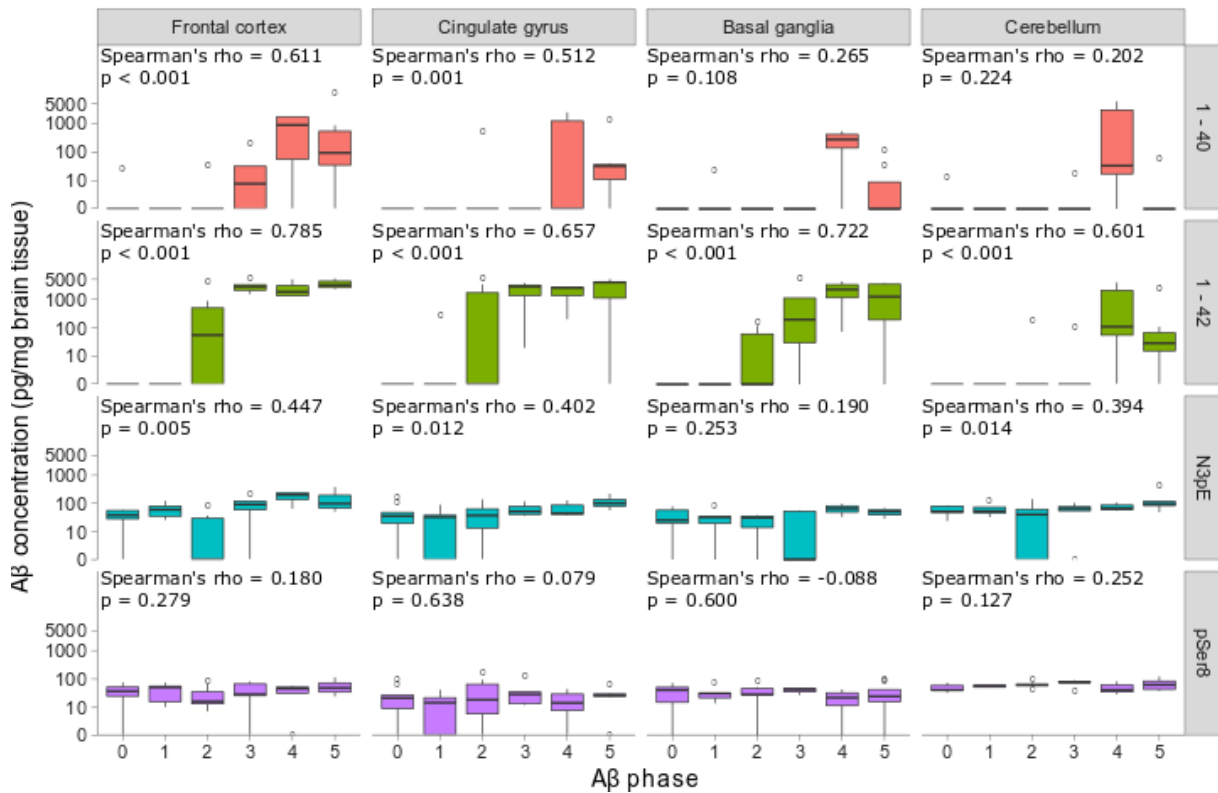
**Supplementary figures and tables:**

**Suppl. Fig. 1:** Biochemical analysis of A $\beta$ , A $\beta_{N3pE}$ , and A $\beta_{pSer8}$  in the human brain among A $\beta$  phases 0-5 using sandwich enzyme-linked immunoassays (ELISA) and western blotting. **a:** Study design of the ELISA and immunohistochemical analysis of human brain tissue from non-AD, p-preAD, and symAD cases. Frozen tissue samples from frontal cortex (Brodmann area 6), cingulate gyrus (Brodmann area 24), putamen (basal ganglia), and cerebellum was taken for biochemical analysis of A $\beta$ . **b:** Prevalence of A $\beta_{1-40}$ , A $\beta_{1-42}$ , A $\beta_{N3pE}$ , and A $\beta_{pSer8}$  as detected by ELISAs of brain homogenates from the mentioned brain regions in cases with A $\beta$  phases 0-5. demonstrated in box and whisker plots. Spearman's correlation analysis between the A $\beta$  phases and the respective ELISA measures has been carried out (n = 38). **c.** Representative standard curves of the sandwich ELISAs targeting A $\beta_{1-40}$ , A $\beta_{1-42}$ , A $\beta_{N3pE}$ , and A $\beta_{pSer8}$ . **d.** Study design of western blot analysis of human brain tissue from non-AD, p-preAD, and symAD cases. Frozen tissue samples from frontal cortex (Brodmann area 6), cingulate gyrus (Brodmann area 24), putamen (basal ganglia), and cerebellum was taken for biochemical analysis of A $\beta$  in the soluble, dispersible, SDS, and FA fraction. **e.** Representative western blots depicting the presence/absence of A $\beta$ , A $\beta_{N3pE}$ , and A $\beta_{pSer8}$ . The 4kDa band is indicated in each blot. The case numbers correspond to Suppl. Tab. 1. A correlation analysis of A $\beta$  loads with the respective A $\beta$  ELISA measurements as well as an association analysis of western blot positive/negative cases with the respective A $\beta$  loads and ELISA measurements is shown in Suppl. Tab. 7.

**a. ELISA and immunohistochemical analysis of human brain tissue from non-AD, p-preAD, and symAD cases**

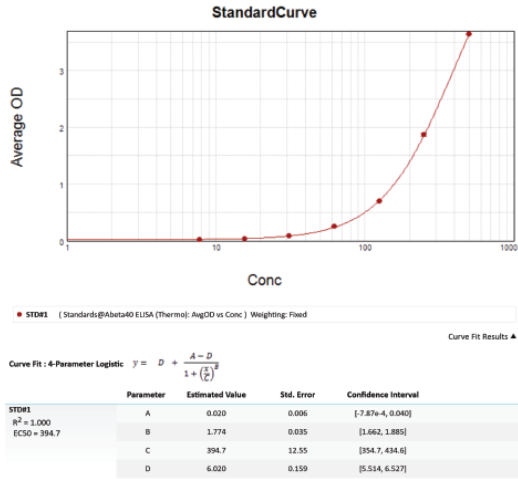


**b. Quantification of Aβ<sub>1-40</sub>, Aβ<sub>1-42</sub>, Aβ<sub>N3pE</sub>, Aβ<sub>pSer8</sub> in human brain lysates among the different Aβ phases**

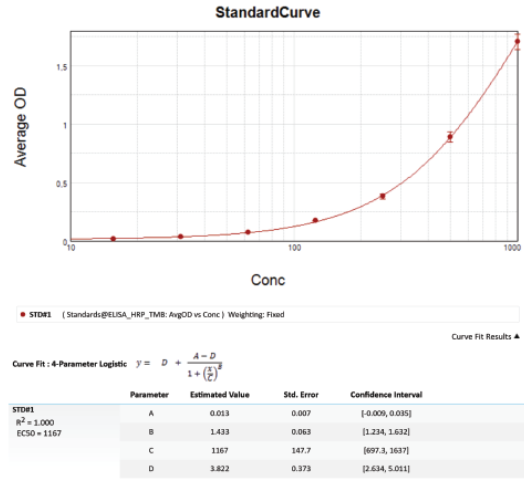


c. Representative standard curves of  $A\beta_{1-40}$ ,  $A\beta_{1-42}$ ,  $A\beta_{N3pE}$ ,  $A\beta_{pSer8}$  sandwich ELISAs

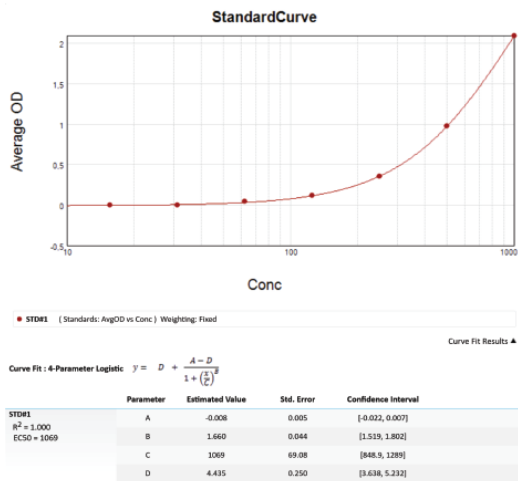
Standard Curve for  $A\beta_{1-40}$



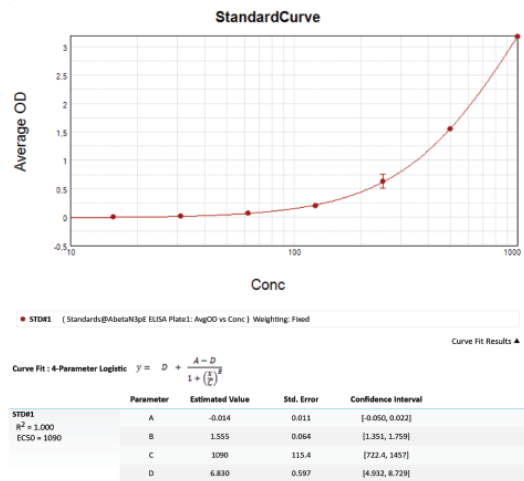
Standard Curve for  $A\beta_{1-42}$



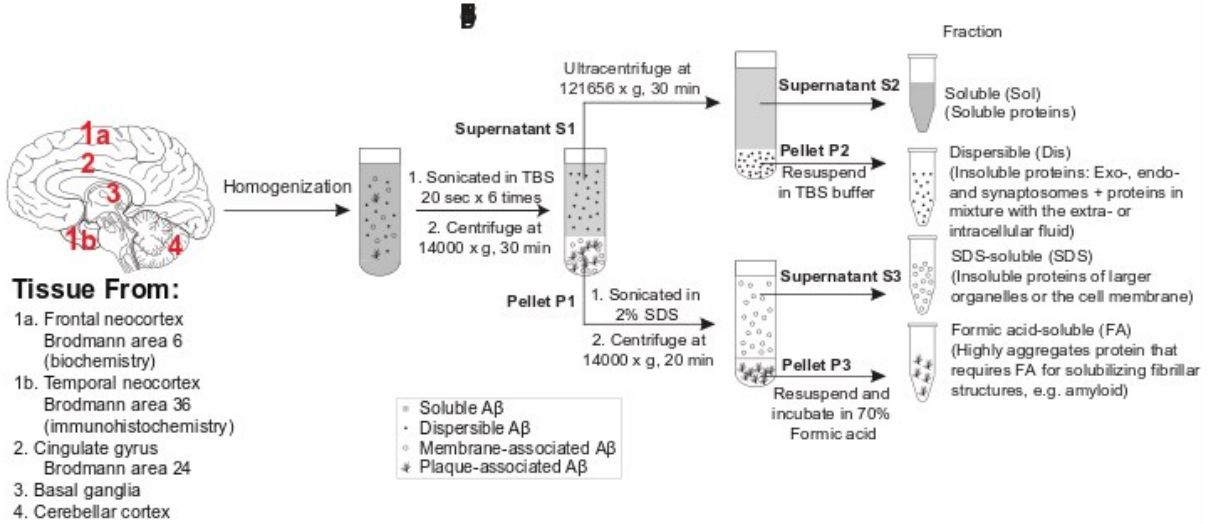
Standard Curve for  $A\beta_{pSer8}$



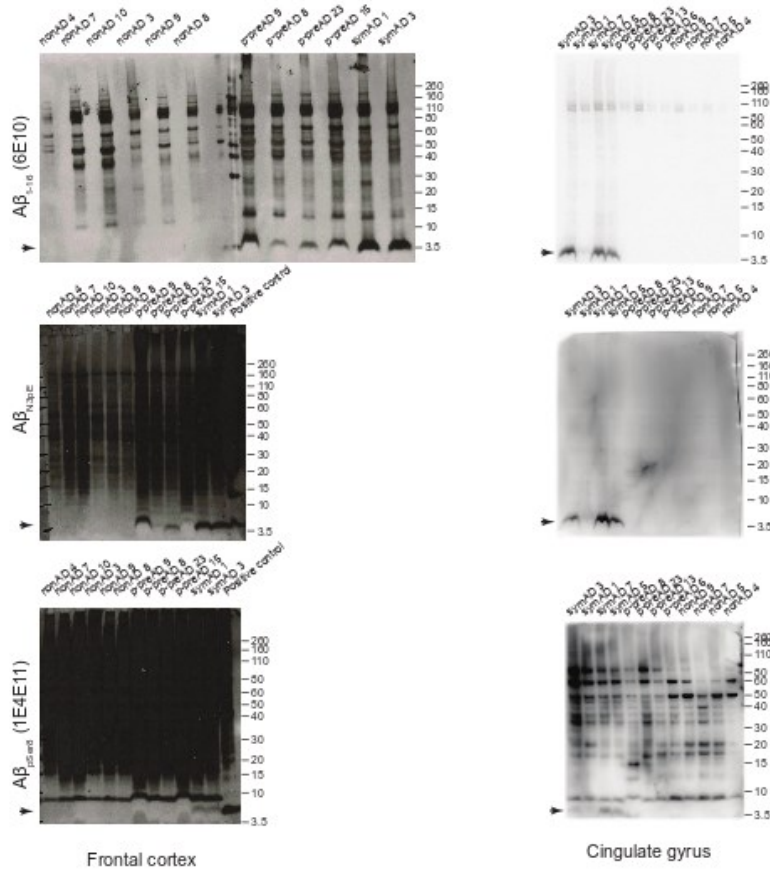
Standard Curve for  $A\beta_{N3pE}$



**d. Biochemical analysis of human brain tissue from non-AD, p-preAD, and symAD cases**

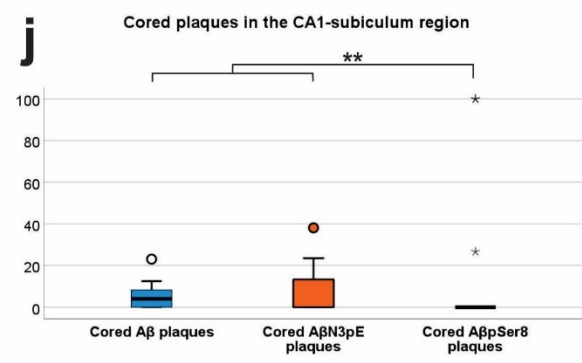
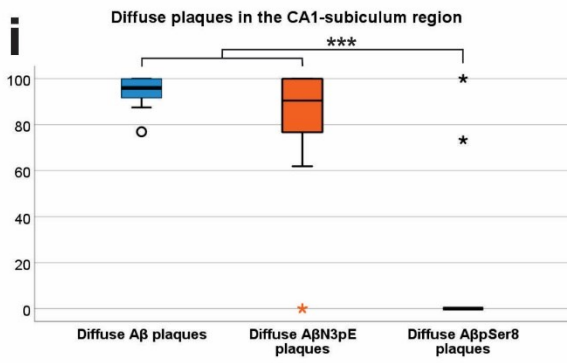
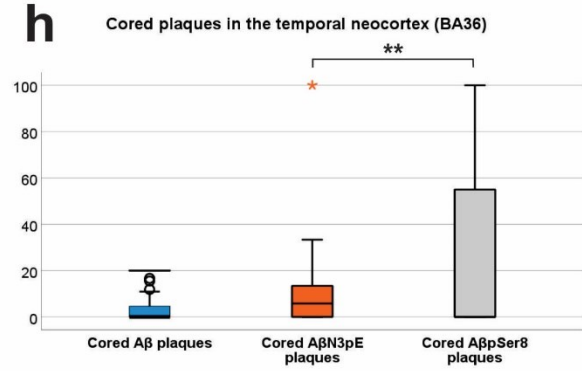
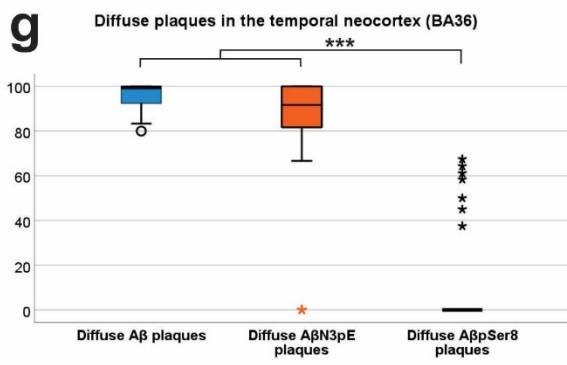
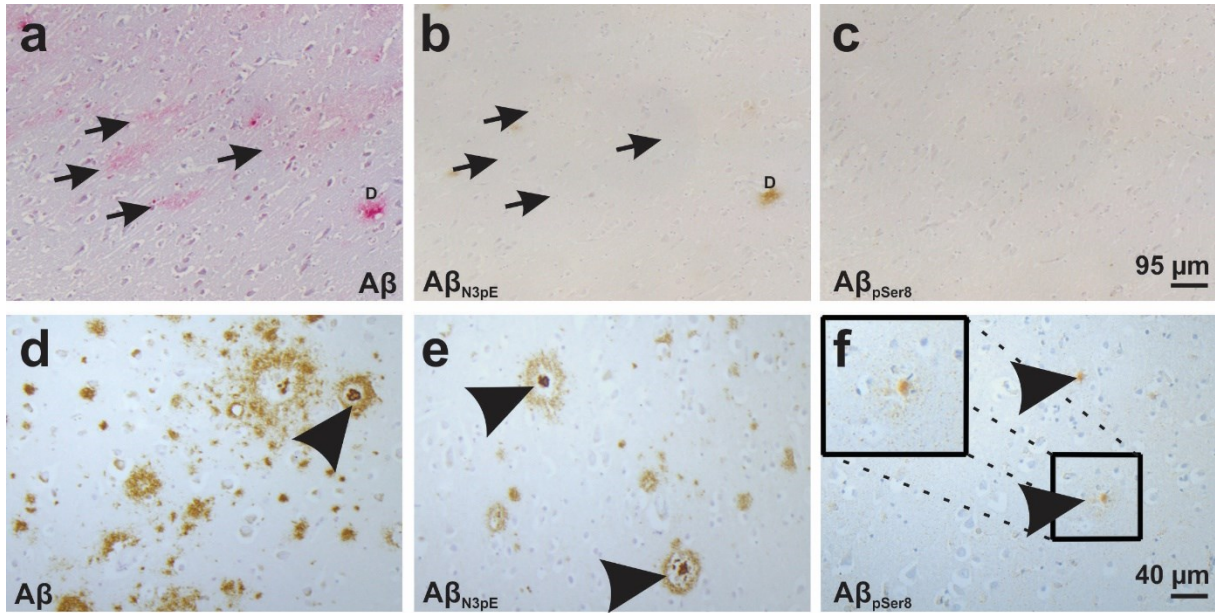


**e. Biochemical detection of A $\beta$ , A $\beta$ <sub>N3pE</sub>, A $\beta$ <sub>pSer8</sub> in human brain lysates among the different A $\beta$  phases**

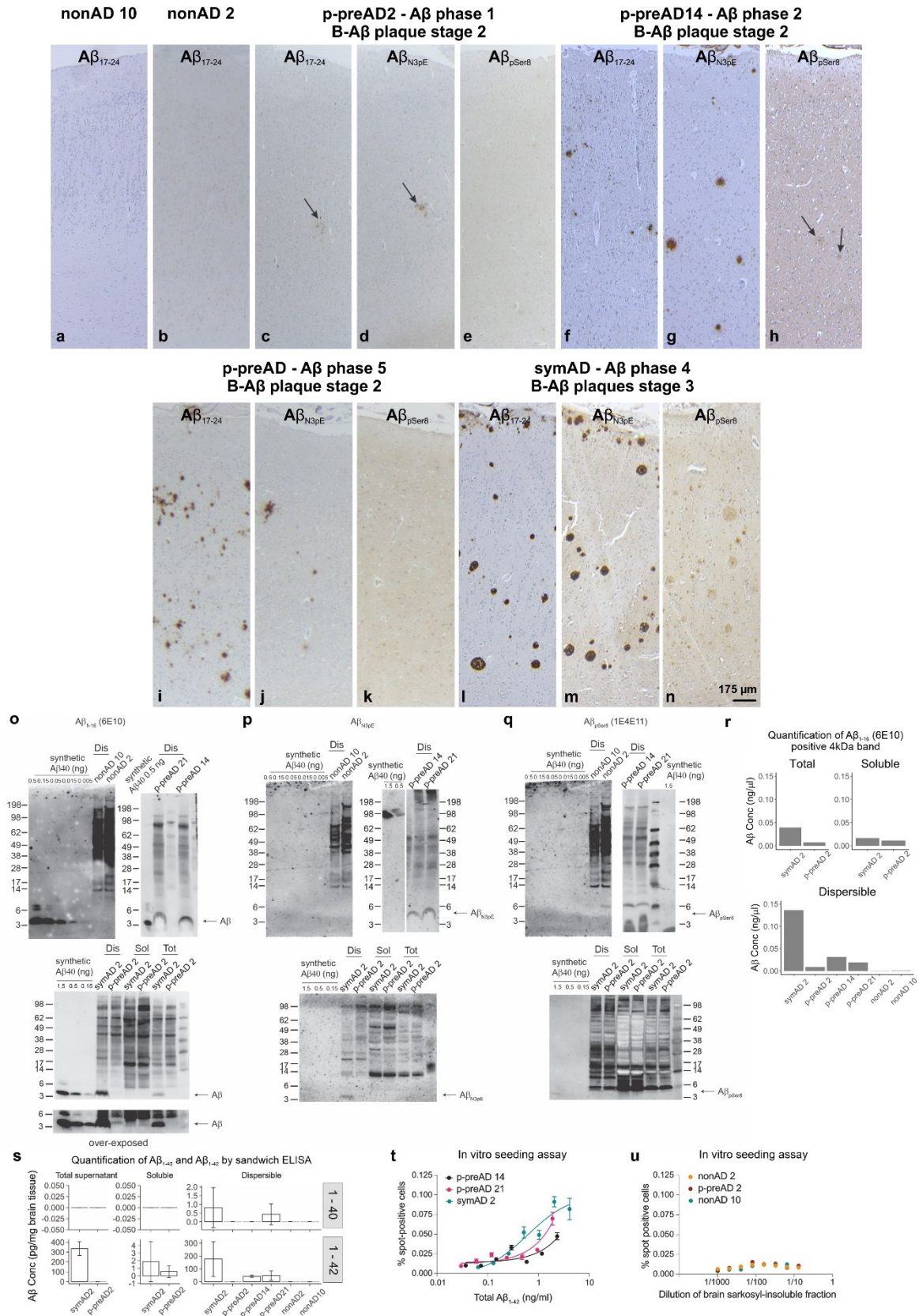


**Suppl. Fig. 2:** Presence/absence of  $A\beta$ ,  $A\beta_{pN3pE}$ , and  $A\beta_{pSer8}$  in different plaque types. **a-c** Fleecy amyloid in the subicular region: In addition to diffuse plaques (D) fleecy amyloid can be visualized with antibodies against  $A\beta_{17-24}$  (**a**: arrows) but not with antibodies against  $A\beta_{N3pE}$  (**b**: arrows) and  $A\beta_{pSer8}$  (**c**). **d-f**: Antibodies raised against  $A\beta_{17-24}$  (**d**) and  $A\beta_{N3pE}$  (**e**) stained diffuse and cored plaques in significant amounts in the temporal neocortex (Brodmann area 36) whereas anti- $A\beta_{pSer8}$  mainly stained cored plaques (**f**). **g-j**: Quantification of the percentages of plaques (diffuse (**g**, **i**) and cored plaques (**h**, **j**)) stained with a given antibody in the temporal cortex (Brodmann area 36) (**g**, **h**) and in the CA1/subiculum regions (**i**, **j**) shows that anti- $A\beta$  and anti- $A\beta_{N3pE}$  antibodies mainly stained diffuse whereas cored plaques represented the minority of plaques positive for these antibodies. In contrast, anti- $A\beta_{pSer8}$  mainly stained cored plaques and only very small amounts of diffuse plaques indicating that the biochemical maturation of  $A\beta$  aggregates goes hand in hand with the maturation from fleecy amyloid to diffuse and later to cored plaques. However, only a minority of the cored plaques exhibited  $A\beta_{pSer8}$ . For this analysis, all cases exhibiting  $A\beta$ -positive plaques in the respective regions were integrated (temporal cortex:  $n = 34$ ; CA1/subiculum:  $n = 23$ ). The data are presented as box and whisker plots. Statistical analysis was carried out with the Cochran Q test corrected for multiple testing by Bonferroni correction: \*\* =  $p < 0.01$ ; \*\*\*  $p < 0.001$ . See also Suppl. Tab. 2. Calibration bar in **c** (valid for **a-c**); calibration bar in **f** (valid for **d-f**).

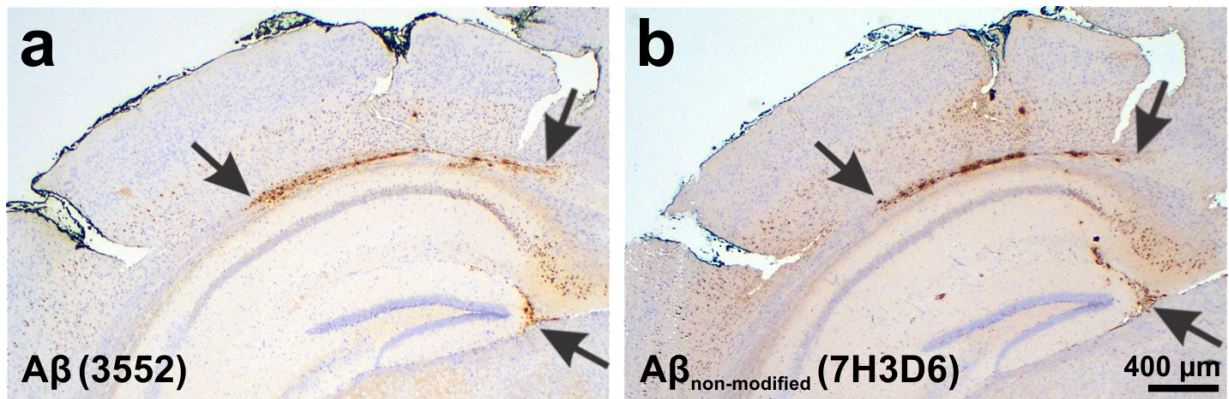




**Suppl. Fig. 3:** Characterization of injection material from human occipital cortex extracts. **a-n:** Representative histopathological sections of all six cases used for the preparation of A $\beta$  seeds. The occipital cortex stained with anti-A $\beta_{17-24}$  (**a, b, c, f, i, l**), anti-A $\beta_{N3pE}$  (**d, g, j, m**), and anti-A $\beta_{pSer8}$  (**e, h, k, n**) is depicted. Arrows indicate single plaques seen in the cortex. The non-AD cases show no A $\beta$  plaques. Therefore, only anti-A $\beta_{17-24}$ -stained sections are depicted. **o-q:** Total supernatant, soluble and dispersible fractions were produced by subsequent centrifugation steps (Fig. 2A). Western blot was performed to analyze A $\beta$  (**o**), A $\beta_{N3pE}$  (**p**) and A $\beta_{pSer8}$  (**q**) in the seeds. The quantification of **o** is shown in **r**. Each bar in **r** indicates one individual brain lysate for injection. **s:** A $\beta_{1-40}$ , A $\beta_{1-42}$  content in the fractions of occipital extracts. The quantification was carried out by sandwich ELISAs in duplicates as demonstrated by the range of the two measurements per case. **t** and **u:** In vitro A $\beta$  seeding assay. Biosensor mCherry-A $\beta_{1-42}$  HEK293T cells were transfected with brain sarkosyl-insoluble fractions and incubated for 72h. A $\beta$  seeding was calculated by counting the fraction of cells containing mCherry-intensive spots as a function of the total A $\beta_{42}$  concentration on the cells (**t**). For the cases of which total A $\beta_{42}$  was below the detection level of the ELISA, the percentage of spot-positive cells was plotted as a function of the dilution of the brain sarkosyl-insoluble fractions on the cells (**u**). Data are represented separately for each case as mean values  $\pm$  SEM (n = 8 independent wells/case). SymAD 2 shows the highest A $\beta$  seeding-potency with an EC50 of 0.6083 ng/ml. Statistical analysis of the data presented in **r-u** has not been performed since they only demonstrate the characterization of the lysates from the individual cases injected into the animals.



**Suppl. Fig. 4:** Head-to-head comparison of sections from a mouse receiving seeds from the dispersible fraction of case p-preAD 14 for immunostaining with anti-A $\beta$  (3552) (**a**) and an antibody that specifically detects non-truncated A $\beta$  without phosphorylation of Ser8 (anti-A $\beta_{\text{non-modified}}$ ; 7H3D6)<sup>11</sup> (**b**). Both antibodies stained similar amounts of A $\beta$  in consecutive sections (arrows in **a** and **b**) indicating the A $\beta$  negative for A $\beta_{\text{pSer8}}$  and A $\beta_{\text{N3pE}}$  represents mainly non-modified forms of A $\beta$ . Fig. 4 B-E depict only very few A $\beta_{\text{N3pE}}$  and A $\beta_{\text{pSer8}}$  in this mouse.



**Suppl. Tab. 1:** List of cases. **a.** List of cases used for maturation analysis. Abbreviations: AGD = argyrophilic grain disease; ALS = amyotrophic lateral sclerosis; AML = acute myeloid leukemia; CBD = cortico basal degeneration; CDR = clinical dementia rating score; CERAD = neuritic plaque score according to the consortium to establish a registry for AD; DLB = dementia with Lewy bodies; FTLT-DTP = frontotemporal lobar degeneration with transactive response DNA-binding protein TDP43 pathology; NIA-AA = Degree of AD neuropathological changes according to the recommendations of the National Institute of Aging and the Alzheimer's Association; PART = primary age-related tauopathy; SVD = cerebral small vessel disease; SVE = subcortical vascular encephalopathy; VD = vascular dementia. # = These AD cases fulfilled the DSM IV criteria for dementia, CDR-scores were not determined, WB = western blot, FC = frontal cortex, CG = cingulate gyrus, BG = basal ganglia, CE = cerebellum, n.d. = no data. \* This case was not included in the histological analysis due missing cerebellum sections. **b.** List of cases used for seed preparation for injections.



## a. List of cases used for maturation analysis.

Case No.	Age	Sex	Neuropathological diagnosis	CDR	A $\beta$ phase	Braak NFT stage	CERAD	NIA-AA	B-A $\beta$ stage	B-A $\beta$ plaque stage	CAA stage	PMI/hr	WB and/or ELISA
nonAD 1	60	m	non-AD, Frontal pole defect, old lacunar infarct basal ganglia right, multiple hemorrhagic infarcts right hemisphere, SVD	0	0	0	0	0	0	0	0	24	FC, CG, BG, CE
nonAD 2	45	m	non-AD	0	0	0	0	0	0	0	0	24	FC, CG, BG, CE
nonAD 3	35	m	non-AD, limbic encephalitis	0	0	0	0	0	0	0	0	72	FC, CG, BG, CE
nonAD 4	58	f	non-AD, SVD	0	0	0	0	0	0	0	0	24	FC, CG, BG, CE
nonAD 5	66	m	non-AD, PART, fresh intracerebral hemorrhage right hemisphere	0	0	1	0	0	0	0	0	72	FC, CG, BG, CE
nonAD 6	71	f	non-AD, PART, old microinfarct frontal left hemisphere	0	0	1	0	0	0	0	0	72	FC, CG, BG, CE
nonAD 7	46	m	non-AD, PART	0	0	1	0	0	0	0	0	29	FC, CG, BG, CE
nonAD 8	57	m	non-AD, PART	0	0	1	0	0	0	0	0	144	FC, CG, BG, CE
nonAD 9	59	m	non-AD, PART	n.d.	0	1	0	0	0	0	0	24	FC, CG, BG, CE
p-preAD 1	72	f	old infarct pons, fresh macro- and microinfarcts centroparietal left	0	1	1	0	1	n.d.	1	0	13	/
p-preAD 2	69	f	p-preAD, SVD	0	1	1	0	1	0	2	0	24	FC, CG, BG, CE
p-preAD 3	53	m	p-preAD, SVD	0	1	1	0	1	0	2	0	48	FC, CG, BG, CE
p-preAD 4	78	f	p-preAD, SVE, CBD	3	1	1	0	1	0	2	0	48	FC, CG, BG, CE
p-preAD 5	73	f	p-preAD, SVD	0	1	2	0	1	3	2	0	120	FC, CG, BG, CE
p-preAD 6	72	f	p-preAD	0	1	2	0	1	0	3	0	24	FC, CG, BG, CE
p-preAD 7	72	m	p-preAD, neuromyelitis optica, paraganglioma	0	2	1	0	1	1	2	0	24	FC, CG, BG, CE
p-preAD 8	68	f	p-preAD, SVD	0	2	1	0	1	2	2	0	96	FC, CG, BG, CE
p-preAD 9	64	m	p-preAD, SVD, thalamic infarct	0	2	1	0	1	2	2	0	48	FC, CG, BG, CE
p-preAD 10	73	f	p-preAD, multiple olf infarcts, SVD, CAA	n.d.	2	1	0	1	2	3	0	24	FC, CG, BG, CE
p-preAD 11	86	m	p-preAD, partial infarct in the territory of the left middle cerebral artery, CA1 microinfarct left	0.5	2	2	0	1	n.d.	1	0	24	/
p-preAD 12	73	f	p-preAD, SVD	0	2	2	0	1	0	2	0	n.d.	FC, CG, BG, CE
p-preAD 13	75	m	p-preAD, multiple infarcte (thalamus, midbrain, parietal), old microinfarct CA1 left, lymphocytic meningoencephalitis	0	2	2	0	1	0	2	0	24	FC, CG, BG, CE
p-preAD 14	71	m	p-preAD, SVD, CAA	0	2	2	1	1	2	3	2	n.d.	FC, CG, BG, CE
p-preAD 15	82	f	p-preAD, cerebral carcinoma metastasis, cerebral microinfarcts	n.d.	3	1	1	1	2	3	2	24	FC, CG, BG, CE
p-preAD 16	68	f	p-preAD, cerebral microabscesses, pneumonia	0	3	2	0	1	2	3	2	120	FC, CG, BG, CE
p-preAD 17	84	f	p-preAD, SVD, capillary teleangiectasia in the pons	0	3	2	0	1	2	3		n.d.	/
p-preAD 18	78	f	p-preAD	0	3	2	0	1	2	3	1	72	FC, CG, BG, CE
p-preAD 19	77	f	FTLD-TDP, SVD, fresh bleeding pons	3	3	3	1	2	0	3	0	n.d.	FC, CG, BG, CE
p-preAD 20	77	f	p-preAD, old infarct (basal ganglia)	0	4	2	0	1	3	3	0	48	FC, CG, BG, CE
p-preAD 21	71	f	p-preAD, SVD	0	5	2	0	1	2	2	2	120	FC, CG, BG, CE
p-preAD 22	74	m	p-preAD, SVD, CAA	0	5	3	1	2	3	3	2	48	FC, CG, BG, CE
p-preAD 23*	67	f	normal brain	n.d.	2	2	0	1	2	2	0	96	FC, CG, BG, CE
p-preAD 24	71	m	brain infarcts, argyrophilic grain disease, anterior and middle cerebral artery aneurysms	0	3	1	0	1	n.d.	1	0	72	/
symAD 1	75	f	AD, subdural hematoma, multiple intracerebral hemorrhages in the context of AML, null-cell-adenoma of the pituitary gland	0.5	3	3	1	2	3	3	1	48	FC, CG, BG, CE
symAD 2	79	f	AD#, old microinfarct parietal right hemisphere	n.d.	4	4	2	2	3	3	2	48	FC, CG, BG, CE

symAD 3	84	m	AD, ALS, AGD, SVE	3	4	4	2	2	3	3	2	72	FC, CG, BG, CE
symAD 4	64	f	AD*, SVD	n.d.	5	4	2	2	3	3	1	24	FC, CG, BG, CE
symAD 5	78	m	AD, VD, Meningioma WHO-grade 2	3	5	4	1	2	3	3	2	48	FC, CG, BG, CE
symAD 6	83	m	AD, CAA, intracerebral hemorrhage, cerebellar infarct right, fresh microinfarct frontal left, brain edema	1	5	4	2	2	3	3	2	72	FC, CG, BG, CE
symAD 7	72	f	AD, cerebral carcinoma metastasis, microangiopathy, lacunar thalamic infarct	1	5	4	2	2	3	3	1	12	FC, CG, BG, CE
symAD 8	72	f	AD	3	5	6	3	3	3	3	1	24	FC, CG, BG, CE
symAD 9	84	m	AD, DLB, FTLD-TDP	3	5	6	3	3	3	3	2	120	FC, CG, BG, CE
SymAD10	68	f	AD	1	5	6	2	3	n.d.	3	1	120	/
SymAD11	82	m	AD	2	5	3	2	2	n.d.	3	2	72	/
SymAD12	81	f	AD, lacunar infarct in the pons	3	5	5	1	2	n.d.	3	1	48	/

### b. List of cases used for seed preparation for injections.

Case No.	Age	Sex	Neuropathological diagnosis	CDR	A $\beta$ phase	Braak NFT stage	CERAD	NIA-AA	B-A $\beta$ stage	B-A $\beta$ plaque stage	CAA stage	PMI/hr
nonAD 10	1	m	n.d.	n.d.	0	0	0	0	0	0	0	48
nonAD 2	45	m	non-AD	0	0	0	0	0	0	0	0	24
p-preAD 2	69	f	p-preAD, SVD	0	1	1	0	1	0	2	0	24
p-preAD 14	71	m	p-preAD, SVD, CAA	0	2	2	1	1	2	3	2	n.d.
p-preAD 21	71	f	p-preAD, SVD	0	5	2	0	1	1	2	2	120
symAD 2	79	f	AD#, old microinfarct parietal right hemisphere	n.d.	4	4	2	2	3	3	2	48

**Suppl. Tab. 2:** Maturation of A $\beta$  aggregates in different plaque types. Percentages of cases exhibiting A $\beta$ , A $\beta_{N3pE}$ , and A $\beta_{pSer8}$  in distinct plaque types. In this context, 100% was set for the A $\beta$  form that was present in all cases with a given plaque type in the respective region.

a. Percentages of cases with A $\beta$ , A $\beta_{N3pE}$ , and A $\beta_{pSer8}$  -positive plaques

<b>Percentage of cases (100% is set for the A<math>\beta</math> form that is present in all cases with a given type of A<math>\beta</math> plaques)</b>			
	<b>A<math>\beta</math></b>	<b>A<math>\beta_{N3pE}</math></b>	<b>A<math>\beta_{pSer8}</math></b>
Presubicular lake-like amyloid	100	80	6,67
Subpial band-like amyloid (BA36)	100	93,75	33,33
Diffuse plaques (BA36) - presence	100	86,67	23,08
Cored plaques (BA36) - presence	90	100	70
Diffuse plaques (CA1/subiculum) - presence	100	82,61	8,70
Cored plaques (CA1/subiculum) - presence	100	91,67	25
Fleecy amyloid (CA1/subiculum)	100	0	0

b. Statistical comparison among the prevalence of A $\beta$ , A $\beta_{N3pE}$ , and A $\beta_{pSer8}$  in the distinct plaque types by Cochran Q-test corrected for multiple testing using the Bonferroni method.

Presubicular lake-like amyloid	A $\beta$ and A $\beta_{N3pE}$ > A $\beta_{pSer8}$ ; $p \leq 0.002$
Subpial band-like amyloid (BA36)	A $\beta$ and A $\beta_{N3pE}$ > A $\beta_{pSer8}$ ; $p \leq 0.001$
Diffuse plaques (BA36)	A $\beta$ and A $\beta_{N3pE}$ > A $\beta_{pSer8}$ ; $p \leq 0.001$
Cored plaques (BA36)	A $\beta_{N3pE}$ > A $\beta_{pSer8}$ ; $p = 0.008$
Diffuse plaques (CA1/subiculum)	A $\beta$ and A $\beta_{N3pE}$ > A $\beta_{pSer8}$ ; $p < 0.001$
Cored plaques (CA1/subiculum)	A $\beta$ and A $\beta_{N3pE}$ > A $\beta_{pSer8}$ ; $p \leq 0.003$
Fleecy amyloid (CA1/subiculum)	A $\beta$ > A $\beta_{N3pE}$ and A $\beta_{pSer8}$ ; $p \leq 0.043$



**Suppl. Tab. 3:** Statistical analysis. **a.** Kruskal Wallis H test (2-sided) comparing differences in the seed-induced expansion (hAP scores) and load (A $\beta$  loads) of three A $\beta$  species between mice receiving soluble, dispersible and total fractions obtained from cases p-preAD 2 and symAD2. No differences in the respective A $\beta$  loads and hAP-scores when comparing the seeding effects among the soluble, dispersible and total fraction (n = 18 mice per case (6 per fraction)). **b.** Spearman correlation (two-tailed) between human case AD-related measurements and APP23 mouse (host) A $\beta$  seeding-related measurements. **c.** A non-parametric Friedman test (2-sided) of differences among the expansion (hAP scores) and load (A $\beta$  loads) of three A $\beta$  species.

**a.**

	hAP scores			A $\beta$ loads		
	<i>A<math>\beta</math></i>	<i>A<math>\beta</math><sub>N3pE</sub></i>	<i>A<math>\beta</math><sub>pSer8</sub></i>	<i>A<math>\beta</math></i>	<i>A<math>\beta</math><sub>N3pE</sub></i>	<i>A<math>\beta</math><sub>pSer8</sub></i>
<i>Soluble A<math>\beta</math> vs. Dispersible A<math>\beta</math> vs. Total A<math>\beta</math> p-preAD 2</i>	p = 0.625	p = 0.053	p = 1	p = 0.980	p = 0.120	p = 1
<i>Soluble A<math>\beta</math> vs. Dispersible A<math>\beta</math> vs. Total A<math>\beta</math> symAD 2</i>	p = 0.983	p = 0.819	p = 0.637	p = 0.224	p = 0.739	p = 0.706



c.

Friedman two way analysis of variance by rank		
Pair-wise comparison (A $\beta$ loads)	p value	adjusted p value (Bonferroni correction for multiple tests)
A $\beta$ - A $\beta$ <sub>N3pE</sub>	<0.001	<0.001
A $\beta$ - A $\beta$ <sub>pSer8</sub>	< 0.001	<0.001
A $\beta$ <sub>N3pE</sub> - A $\beta$ <sub>pSer8</sub>	0.061	0.182
Pair-wise comparison (hAP score)	p value	adjusted p value (Bonferroni correction for multiple tests)
A $\beta$ - A $\beta$ <sub>N3pE</sub>	0.001	0.002
A $\beta$ - A $\beta$ <sub>pSer8</sub>	< 0.001	<0.001
A $\beta$ <sub>N3pE</sub> - A $\beta$ <sub>pSer8</sub>	0.037	0.112

**Suppl. Tab. 4:** The overview of the Bregma coordinates that were used for the AP scoring.

Section A-P score	Position Allen Brain Atlas	Section n° Atlas	A-P coordinate from Bregma
1	mousebrain_241	Coronal level 61	-0.655
2	mousebrain_257	Coronal level 65	-1.055 mm
3	mousebrain_265	Coronal level 67	-1.255 mm
4	mousebrain_273	Coronal level 69	-1.455 mm
5	mousebrain_289	Coronal level 73	-1.855 mm
6	mousebrain_301	Coronal level 76	-2.155 mm
7	mousebrain_309	Coronal level 78	-2.355 mm
8	mousebrain_317	Coronal level 80	-2.555 mm
9	mousebrain_330	Coronal level 83	-2.98 mm
10	mousebrain_342	Coronal level 86	-3.28 mm
11	mousebrain_349	Coronal level 88	-3.455 mm
12	mousebrain_358	Coronal level 90	-3.68 mm

**Suppl. Tab. 5:** List of antibodies.**IHC = immunohistochemistry, WB = western blotting.**

Antibody	Antigen	Host	Clone	Concentration IHC	Concentration ELISA	Concentration WB	Pretreatment for IHC	Source	Sensitivity in WB	Purpose of Use
anti-A $\beta$ <sub>17-24</sub>	A $\beta$ 17-24	mouse	4G8	1/5000			formic acid	Covance, USA		Determination of A $\beta$ phases, A $\beta$ MTL phase, B-A $\beta$ plaque stages, A $\beta$ load, and CAA. This antibody detects full-length as well as N-terminal truncated forms of A $\beta$ <sub>40/42</sub> .
anti-A $\beta$ <sub>1-16</sub>	A $\beta$ 1-16	mouse	6E10			1/1000	n.a.	Covance, USA	5 ng/ml <sup>13</sup>	Determination of biochemical A $\beta$ levels and B-A $\beta$ stage. This antibody detects full-length forms of A $\beta$ <sub>40/42</sub> .
Anti-A $\beta$ (3552)	A $\beta$ <sub>1-40</sub> (this antibody is not C-terminus specific)	Rabbit	polyclonal	1/1000			formic acid	<sup>14</sup> gift Dr. Willem, Munich, Germany		Determination of A $\beta$ load, and hA $\beta$ -score in mice. This antibody detects full-length as well as N-terminal truncated forms of A $\beta$ .
anti-A $\beta$ <sub>N3pE</sub>	A $\beta$ N3pE	rabbit	polyclonal	1/100		1/500	formic acid, heat pretreatment at pH6	IBL, Japan	~20 ng/ml <sup>15</sup>	Determination of B-A $\beta$ stage, B-A $\beta$ plaque stages, biochemical levels of A $\beta$ <sub>N3pE</sub> , A $\beta$ <sub>N3pE</sub> load, and hAPA $\beta$ <sub>N3pE</sub> score in either mouse or man
anti-A $\beta$ <sub>N3pE</sub> (J8)	A $\beta$ N3pE	mouse	J8		1/500			<sup>10</sup> gift Fraunhofer Institute Halle, Germany		Determination of A $\beta$ <sub>N3pE</sub> concentration in human brain lysates.
anti-A $\beta$ <sub>pSer8</sub>	A $\beta$ pSer8	mouse	1E4E11	1/5	1/500	1/50	formic acid, heat pretreatment at pH6	<sup>11</sup> gift Prof. Walter, Bonn, Germany	25 ng/ml <sup>11</sup>	Determination of B-A $\beta$ stage, B-A $\beta$ plaque stages, A $\beta$ <sub>pSer8</sub> concentration, biochemical levels of A $\beta$ <sub>pSer8</sub> , A $\beta$ <sub>pSer8</sub> load, and hAPA $\beta$ <sub>pSer8</sub> score in either mouse or man
Anti-A $\beta$ (non-modified)	A $\beta$ Ser8, not truncated	rat	7H3D6	1/150			formic acid, heat pretreatment at pH6	<sup>11</sup> gift Prof. Walter, Bonn, Germany		Confirmation of the presence of non-modified A $\beta$ , i.e., non-truncated A $\beta$ with Ser8 <sup>11</sup>
anti-abnormal $\tau$ protein	phosphorylated $\tau$ (pSer 202 and pThr205)	mouse	AT8	1/1000			-	Thermo-Scientific, USA		Assessment of Braak NFT stages, neuritic plaques (CERAD scores were based on these stainings) and accompanying $\tau$ pathology

**Suppl. Tab. 6:** Summary of the body weight of mice included in this study.

Group	Median (min - max)	
	Before the surgery	Endpoint
p-preAD2 soluble fraction	18.15 (17 - 19.3)	22.55 (20.6 - 23.5)
p-preAD2 dispersible fraction	19.45 (17.7 - 21.1)	23.15 (22 - 25.8)
p-preAD2 total supernatant fraction	19.45 (17.8 - 22.2)	22.7 (22.1 - 23.8)
symAD2 soluble fraction	19.1 (17.4 - 21.2)	22.3 (21.8 - 25.5)
symAD2 dispersible fraction	19.55 (19.2 - 20.6)	23.2 (21 - 24.5)
symAD2 total supernatant fraction	19.6 (17.9 - 22.5)	23.85 (23.1 - 29.8)
PBS	19.5 (15.9 - 20.2)	22.7 (22.1 - 24.3)
nonAD10 dispersible fraction	19.3 (19.1 - 19.8)	25.1 (24.1 - 25.7)
nonAD2 dispersible fraction	18.5 (17.6 - 21.2)	23.6 (22.6 - 26.4)
p-preAD14 dispersible fraction	19.2 (17.5 - 22.5)	22.9 (20 - 28.1)
p-preAD21 dispersible fraction	19.09 (18.59 - 19.9)	24.1 (23.4 - 24.7)

**Suppl. Tab. 7:** Comparison of local A $\beta$ , A $\beta$ <sub>N3pE</sub>, and A $\beta$ <sub>pSer8</sub> detection/quantification by A $\beta$  plaque loads, ELISA measurements, and western blot detection. Only correlations/associations between measurements of the same A $\beta$  species are shown. For western blot analysis, cases were considered as positive if one or more of the four fractions exhibited a 4 kDa A $\beta$  band. n = 38 cases. n.d. = no case with A $\beta$  detected by western blotting.

**a:** Spearman correlations between A $\beta$  plaque loads and ELISA measurements

	<b>A<math>\beta</math><sub>42</sub>-ELISA</b>	<b>A<math>\beta</math><sub>40</sub>-ELISA</b>	<b>A<math>\beta</math><sub>N3pE</sub>-ELISA</b>	<b>A<math>\beta</math><sub>pSer8</sub>-ELISA</b>
<i>Neocortex</i>				
A $\beta$ load	r = 0.723; p < 0.001	r = 0.527; p < 0.001		
A $\beta$ <sub>N3pE</sub> load			r = 0.383; p = 0.017	
A $\beta$ <sub>pSer8</sub> -load				r = 0.309; p = 0.059
<i>Allocortex (cingulate gyrus)</i>				
A $\beta$ load	r = 0.629; p < 0.001	r = 0.414; p = 0.010		
A $\beta$ <sub>N3pE</sub> load			r = 0.397; p = 0.014	
A $\beta$ <sub>pSer8</sub> -load				p = 0.989
<i>Basal ganglia (putamen)</i>				
A $\beta$ load	r = 0.771; p < 0.001	p = 0.521		
A $\beta$ <sub>N3pE</sub> load			p = 0.262	
A $\beta$ <sub>pSer8</sub> -load				p = 0.838
<i>Cerebellar cortex</i>				
A $\beta$ load	r = 0.484; p = 0.002	p = 0.1		
A $\beta$ <sub>N3pE</sub> load			r = 0.461; p = 0.004	
A $\beta$ <sub>pSer8</sub> -load				p = 0.520

**b:** Mann-Whitney U-test comparing western blot-positive and negative cases for A $\beta$ , A $\beta$ <sub>N3pE</sub>, and A $\beta$ <sub>pSer8</sub> among the respective A $\beta$  ELISA measurements.

	<b>A<math>\beta</math><sub>42</sub>-ELISA</b>	<b>A<math>\beta</math><sub>40</sub>-ELISA</b>	<b>A<math>\beta</math><sub>N3pE</sub>-ELISA</b>	<b>A<math>\beta</math><sub>pSer8</sub>-ELISA</b>
<i>Neocortex</i>				
A $\beta$	p < 0.001	p < 0.001		
A $\beta$ <sub>N3pE</sub>			p = 0.022	
A $\beta$ <sub>pSer8</sub>				p = 0.086
<i>Allocortex (cingulate gyrus)</i>				
A $\beta$	p < 0.001	p = 0.012		
A $\beta$ <sub>N3pE</sub>			p = 0.027	
A $\beta$ <sub>pSer8</sub>				p = 0.667
<i>Basal ganglia (putamen)</i>				
A $\beta$	p = 0.013	p = 0.941		
A $\beta$ <sub>N3pE</sub>			p = 0.869	
A $\beta$ <sub>pSer8</sub>				p = 0.141
<i>Cerebellar cortex</i>				
A $\beta$	n.d.	n.d.		
A $\beta$ <sub>N3pE</sub>			n.d.	
A $\beta$ <sub>pSer8</sub>				n.d.

c: Mann-Whitney U-test comparing western blot-positive and negative cases for A $\beta$ , A $\beta$ <sub>N3pE</sub>, and A $\beta$ <sub>pSer8</sub> among the respective A $\beta$  loads.

	<b>A<math>\beta</math>-load</b>	<b>A<math>\beta</math><sub>N3pE</sub>-load</b>	<b>A<math>\beta</math><sub>pSer8</sub>-load</b>
<i>Neocortex</i>			
A $\beta$	p < 0.001		
A $\beta$ <sub>N3pE</sub>		p < 0.001	
A $\beta$ <sub>pSer8</sub>			p < 0.001
<i>Allocortex (cingulate gyrus)</i>			
A $\beta$	p = 0.004		
A $\beta$ <sub>N3pE</sub>		p < 0.001	
A $\beta$ <sub>pSer8</sub>			p < 0.001
<i>Basal ganglia (putamen)</i>			
A $\beta$	p = 0.005		
A $\beta$ <sub>N3pE</sub>		p = 0.025	
A $\beta$ <sub>pSer8</sub>			p = 0.021
<i>Cerebellar cortex</i>			
A $\beta$	n.d.		
A $\beta$ <sub>N3pE</sub>		n.d.	
A $\beta$ <sub>pSer8</sub>			n.d.



## References

1. Thal DR, Rüb U, Orantes M, Braak H. Phases of Abeta-deposition in the human brain and its relevance for the development of AD. *Neurology*. 2002;58:1791-1800.
2. Alafuzoff I, Thal DR, Arzberger T, et al. Assessment of beta-amyloid deposits in human brain: a study of the BrainNet Europe Consortium. *Acta Neuropathol*. Mar 2009;117(3):309-20.
3. Braak H, Alafuzoff I, Arzberger T, Kretschmar H, Del Tredici K. Staging of Alzheimer disease-associated neurofibrillary pathology using paraffin sections and immunocytochemistry. *Acta Neuropathol*. Oct 2006;112(4):389-404.
4. Mirra SS, Heyman A, McKeel D, et al. The Consortium to Establish a Registry for Alzheimer's Disease (CERAD). Part II. Standardization of the neuropathologic assessment of Alzheimer's disease. *Neurology*. 1991;41(4):479-86.
5. Thal DR, Ghebremedhin E, Orantes M, Wiestler OD. Vascular pathology in Alzheimer's disease: Correlation of cerebral amyloid angiopathy and arteriosclerosis / lipohyalinosis with cognitive decline. *J Neuropathol Exp Neurol*. 2003;62(12):1287-1301.
6. Rijal Upadhaya A, Capetillo-Zarate E, Kosterin I, et al. Dispersible amyloid  $\beta$ -protein oligomers, protofibrils, and fibrils represent diffusible but not soluble aggregates: Their role in neurodegeneration in amyloid precursor protein (APP) transgenic mice. *Neurobiol Aging*. 2012;33:2641-2660.
7. Rijal Upadhaya A, Kosterin I, Kumar S, et al. Biochemical stages of amyloid  $\beta$ -peptide aggregation and accumulation in the human brain and their association with symptomatic and pathologically-preclinical Alzheimer's disease. *Brain*. 2014;137:887-903.
8. Thal DR, Ronisz A, Tousseyn T, et al. Different aspects of Alzheimer's disease-related amyloid beta-peptide pathology and their relationship to amyloid positron emission tomography imaging and dementia. *Acta neuropathologica communications*. Nov 14 2019;7(1):178.
9. Mc Donald JM, Savva GM, Brayne C, et al. The presence of sodium dodecyl sulphate-stable Abeta dimers is strongly associated with Alzheimer-type dementia. *Brain*. May 2010;133(Pt 5):1328-41.
10. Hartlage-Rubsamen M, Bluhm A, Piechotta A, et al. Immunohistochemical Evidence from APP-Transgenic Mice for Glutaminyl Cyclase as Drug Target to Diminish pE-Abeta Formation. *Molecules*. Apr 17 2018;23(4)
11. Kumar S, Wirths O, Theil S, Gerth J, Bayer TA, Walter J. Early intraneuronal accumulation and increased aggregation of phosphorylated Abeta in a mouse model of Alzheimer's disease. *Acta Neuropathol*. May 2013;125(5):699-709.
12. Konstantoulea K, Guerreiro P, Ramakers M, et al. Heterotypic Amyloid beta interactions facilitate amyloid assembly and modify amyloid structure. *The EMBO journal*. Dec 17 2022;41(2):e108591.
13. Youmans KL, Tai LM, Kanekiyo T, et al. Intraneuronal Abeta detection in 5xFAD mice by a new Abeta-specific antibody. *Mol Neurodegener*. 2012;7:8. 2012.
14. Page RM, Gutsmedl A, Fukumori A, Winkler E, Haass C, Steiner H. Beta-amyloid precursor protein mutants respond to gamma-secretase modulators. *The Journal of biological chemistry*. Jun 4 2010;285(23):17798-810.
15. Saido TC, Iwatsubo T, Mann DM, Shimada H, Ihara Y, Kawashima S. Dominant and differential deposition of distinct beta-amyloid peptide species, A beta N3(pE), in senile plaques. *Neuron*. Feb 1995;14(2):457-66.